Soft Matter

PAPER

Effect of ionic strength on rheological behavior of polymer-like cetyltrimethylammonium tosylate micellar solutions†

E. R. Macías,[a] F. Bautista,[b] J. H. Pérez-López,[a] P. C. Schulz,[c] M. Gradzielski,[d] O. Manero,[e] J. E. Puig[a] and J. I. Escalante*[f]

The influence of ionic strength on the rheological properties of polymer-like aqueous micellar solutions of cetyltrimethylammonium tosylate (CTAT) containing different salts (KCl, KBr, $(COONa)_2$, K_2SO_4 or K_3PO_4) is investigated. The rheological behavior of the solutions is analyzed above the concentration where a micellar entanglement network is formed, varying surfactant and salt concentration, salt counterion valency and temperature. A *master curve* of the linear viscoelastic properties is obtained by multiple superposition of time, temperature, salt type, and surfactant and salt concentration. Application of the existent kinetic theory provides information suggesting that the micellar solutions are in the *fast breaking* regime (*i.e.*, the relaxation is kinetically controlled) regardless of salt type and concentration. Moreover, these solutions exhibit shear-banding flow with a reduced stress plateau (σ/G_0, being σ and G_0 the shear stress and the plateau modulus, respectively) that increases with salt content and counterion valency. The zero-shear viscosity (η_0) and the main relaxation time (τ_C) diminish with increasing salt content according to a step-like function, in which the number of steps increases with the salt counterion valence. In contrast, G_0 only increases slightly with increasing salt content for the five salts employed. These results are discussed in terms of ionic strength and screening of the electrostatic-interactions caused by the addition of salt. In addition, it was found that the influence of anions on the viscoelastic properties of the polymer-like micelles follows the Hofmeister series commonly encountered in macromolecular and biological systems. This finding opens a challenge for scientists in the experimental and theoretical fields.

Introduction

At concentrations larger than the critical micelle concentration (*cmc*), most surfactants spontaneously form spherical micelles in aqueous solutions; at even higher concentrations, they grow to

[a] Departamento de Ingeniería Química, Universidad de Guadalajara, Boul. M. García Barragán # 1451, Guadalajara, Jal., 44430, México. E-mail: emmarebecamacias@hotmail.com; jperez50@hotmail.com; puigje@hotmail.com

[b] Departamento de Física, Universidad de Guadalajara, Boul. M. García Barragán # 1451, Guadalajara, Jal., 44430, México. E-mail: ferbautistay@yahoo.com

[c] Departamento de Química, Universidad Nacional del Sur, Bahía Blanca, 8000, Argentina. E-mail: pschulz@criba.edu.ar

[d] Stranski-Laboratorium für Physikalische und Theoretische Chemie, Institut für Chemie, Technische Universität Berlin, Straße des 17. Juni 124, Sekr. TC7, D-10623 Berlin, Germany. E-mail: michael.gradzielski@tu-berlin.de

[e] Instituto de Investigaciones en Materiales, UNAM, Apdo. Postal 70-360, México City, DF, 04510, Mexico. E-mail: manero@unam.mx

[f] Departamento de Química, Universidad de Guadalajara, Boul. M. García Barragán # 1451, Guadalajara, Jal., 44430, México. E-mail: escalant@hotmail.com; Tel: +52-33-13785900 ext 7536

yield rod-like micelles at the *cmc* II.[1] The addition of inorganic salts to ionic surfactant solutions screens the repulsions between the charged heads and decreases the concentration at which the transition from spherical to rod-like micelles occurs.[2–7] This transition takes place at even lower concentrations in the presence of organic (hydrotropic) salts or in surfactants with counterions such as salicylate,[3,8–10] tosylate,[11] chlorobenzoate,[12] hydroxyl naphthalene carboxylate,[5,13] and alkyl sulfates[14] without the addition of electrolytes. The intensity of binding to the micelles is a function of the hydrophobicity of the counterion.[13]

Most of the rheological studies of wormlike micellar solutions have been performed with cationic surfactants, such as alkyl-trimethylammonium halides and alkylpyridium halides, or anionic surfactants (sodium dodecyl sulfate), in the presence of inorganic or organic salts, *i.e.*, in highly screened systems.[8,15–19] Some authors have added another inorganic salt, such as NaCl or KBr, to further screen the electrostatic interactions in these surfactant/salt (inorganic or organic)/water micellar systems.[16,20–22] By contrast, the structural and rheological reports on salt-free viscoelastic micellar solutions are scarce. Kern *et al.*[22] investigated the linear viscoelastic behavior of salt-free polymer-like

micellar solutions made with a gemini surfactant as a function of surfactant concentration; they found that for surfactant concentrations larger than the overlapping value, the viscosity increases rapidly and goes through a maximum suggesting micellar growth. Moreover, G_0 exhibits stronger concentration dependence than in the highly screened case.

Kadoma and van Egmond[23] showed the existence of a shear-induced phase transition in a semidilute micellar solution of cetyltrimethylammonium bromide (CTAB) and sodium salicylate (NaSal) in a molar ratio of 1 : 8, at a shear rate of 15 s⁻¹. The induced phase is thought to consist of highly elongated strings oriented in the flow direction as evidenced by tulip-like SALS patterns. These patterns were in qualitative agreement with the Porte model[24] of a structural evolution from an entangled to a multiconnected network as the salt concentration is increased as well as with the flow-induced 1-D gel phase predicted by Turner and Cates.[25] Other authors studied the effect of electrostatic interactions on the viscoelasticity of unscreened and screened polymer-like micelles of cetyltrimethylammonium (CTA⁺) with various hydrophobic counterions.[13,14] One of them, CTA hydroxynaphthalene carboxylate (CTAHCN) exhibits a vesicle to micelle transformation with temperature and strong viscoelasticity at high temperatures.[14]

Our group has studied the phase and rheological behavior of CTA-tosylate (CTAT) in water.[11] This cationic surfactant forms polymer-like micelles in water at low concentrations (15.4 mM).[11,14] Because these micelles can form concentrated entanglement networks even at low concentrations, they exhibit strong nonlinear viscoelastic behavior similar to that of semi-dilute polymer solutions.[11] However, in contrast to most polymer systems, the linear viscoelastic behavior of CTAT micellar solutions in the semi-diluted and concentrated regimes is described by the Maxwell model.[11,26] Moreover, under steady shear, these solutions exhibit shear-banding flow in the concentration range of ca. 0.044 to 0.55 M at 30 °C.[11]

In this paper, the linear as well as the steady and transient nonlinear viscoelastic behaviors of CTAT polymer-like micellar solutions are reported in the presence of a series of inorganic salts (with a mono-, di- or tri-valent counterion), which are investigated and discussed in terms of electrostatic effects and the Hofmeister series. The Hofmeister series accounts for the fact that the binding of counterions at interfaces depends not only on the charge of the counterions but often shows pronounced ion specificity, which renders this effect very important for many phenomena in colloidal and biological science. This series has aroused a lot of scientific attention in recent years because of their relevance in a broad range of fields that include enzyme activity, protein stability and crystallization and ion–macromolecule interactions, among others.[27]

The linear viscoelastic data are analyzed with the Granek–Cates model to determine whether the dynamics of the micelles are kinetically controlled (fast breaking regime) or diffusion-controlled (slow breaking regime)[28] and the nonlinear shear data are compared with the predictions of the BMP model.[29] The relationship between these regimes with the formation of shear banding in steady shear flow as well as the roles of electrostatic and ion-specific interactions are further examined. The aim of this study then was to find systematic correlations between the flow behaviour observed and the type of counterion present.

Results

Fig. 1 reports the reduced zero-shear complex viscosity, $|\eta^*|/|\eta^*|_0$, and the reduced linear moduli, G'/G_0, and G''/G_0, as a function of the reduced frequency, $\omega\tau_C$, measured from 28 to 34 °C, for micellar solutions containing 0.11 M and 0.24 M CTAT and salt (KCl, KBr, K₂SO₄, (COONa)₂ or K₃PO₄) at different salt-to-surfactant molar ratios (C_{SALT}/C_{CTAT} = 0, 0.21, 0.23 and 4.56). η_0, G_0 and τ_C were obtained independently for each solution (Table 1). The solid lines in Fig. 1 are the predictions of the Maxwell model with the value of τ_C obtained from the inverse of the crossover frequency of the elastic (G') and the viscous (G'') moduli. All data collapse into a single line regardless of surfactant concentration, temperature and salt type and concentration. Moreover, the Maxwell model with a single relaxation time predicts remarkably well the data except for the normalized viscous modulus at moderate normalized frequencies ($\omega\tau_C > 1$), as expected from Cates' model.[28] The departures from Maxwell behavior of G'' at higher frequencies can be associated to the breaking time (τ_{break}) of the micelles.[30,31] At even higher normalized frequencies ($\omega\tau_C > 30$), an upturn in G'' is detected, i.e., G'' departs from the Maxwell model, goes through a minimum and then it increases linearly with frequency.[28,31] This upturn in G'' is related to the occurrence of the Rouse and the breathing relaxation modes at high frequencies. Notice that the minimum value of G'' at the upturn (G''_{min}) shifts to lower values of $\omega\tau_C$ with increasing C_{SALT}/C_{CTAT}. Schmitt and Lequeux[32] reported similar results in solutions of polyelectrolytes, presumably due to changes in micellar length and rigidity and in the breaking and recombination processes. For micellar solutions with higher surfactant concentration (0.24 M CTAT in brine), the departure of normalized frequency of the viscous modulus (G''/G_0) from the Maxwell model shifts to higher values (not shown), probably because the micelles become longer as the
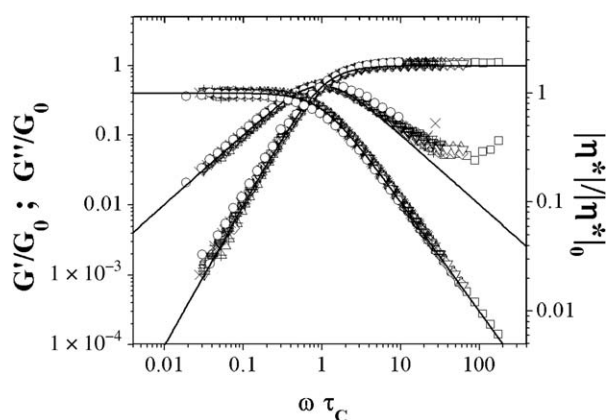

Fig. 1 Reduced linear oscillatory data as a function of reduced frequency for CTAT micellar solutions containing salt; data were taken at various temperatures. C_{CTAT}–C_{SALT}/C_{CTAT} (type of salt)–temperature (°C)_(□) 0.11–0.0–30; (△) 0.11–0.23 (KBr)–30; (◇) 0.11–0.23 (KCl)–30; (▽) 0.11–0.23 (K₂SO₄)–30; (*) 0.11–0.23 (K₃PO₄)–30; (○) 0.11–4.56 (K₂SO₄)–32; (■) 0.24–0.0–30; (▲) 0.24–0.21 (KBr)–30; (◆) 0.24–0.21 (KCl)–30; (▼) 0.24–0.21 (K₂SO₄)–30; (×) 0.24–0.21 (K₃PO₄)–30; (●) 0.24–0.21 (K₂SO₄)–32.

Table 1 Rheological parameters of aqueous micellar solutions containing 0.11 M CTAT and the polyprotic salts used in this work (K_3PO_4, K_2SO_4, (COO Na)$_2$, KBr and KCl) as a function of C_{SALT}/C_{CTAT}

C_{SALT}/C_{CTAT}	K_3PO_4		(COONa)$_2$		K_2SO_4	
	$\eta_0{}^a$/Pa s	τ_C/s	$\eta_0{}^a$/Pa s	τ_C/s	$\eta_0{}^a$/Pa s	τ_C/s
0	102	1.90	100	1.95	125	1.82
9×10^{-6}	104	1.80	103	1.92	127	1.80
4×10^{-4}	103	1.85	100	1.80	122	1.79
6×10^{-4}	103	1.84	100	1.75	122	1.78
1×10^{-3}	92	1.38	96	1.72	120	1.80
2×10^{-3}	82	1.23	96	1.62	119	1.65
3×10^{-3}	78	1.20	95	1.60	119	1.59
9×10^{-3}	80	1.21	94	1.50	101	1.35
0.01	70	1.10	85	1.45	93	1.25
0.02	54	0.85	64	1.11	73	1.12
0.02	45	0.72	58	1.10	61	0.88
0.07	34	0.50	39	0.58	43	0.58
0.14	29	0.46	38	0.60	42	0.60
0.46	27	0.40	35	0.52	39	0.57
0.91	29	0.39	34	0.55	41	0.58
1.37	32	0.38	32	0.48	32	0.42
1.82	27	0.26	28	0.38	28	0.36
3.65	4	0.05	11	0.14	11	0.14
4.56	5	0.06	9	0.11	8	0.10

^{a} In all the cases the apparent viscosity was quite similar to the zero-shear complex viscosity. The value of G_0 can be determined from the relationship, $G_0 = \eta_0/\tau_C$.

C_{SALT}/C_{CTAT}	KBr		KCl	
	$\eta_0{}^a$/Pa s	τ_C/s	$\eta_0{}^a$/Pa s	τ_C/s
0	101	1.94	87	1.68
4×10^{-4}	102	1.90	94	1.70
0.031	70	1.20	92	1.20
0.046	64	1.09	80	1.03
0.091	49	0.84	65	0.85
0.207	33	0.59	49	0.70
0.228	34	0.57	47	0.61
0.684	23	0.33	35	0.41
0.912	21	0.32	30	0.35
1.053	22	0.34	28	0.33
1.823	20	0.27	26	0.32
4.558	18	0.29	26	0.38
8.288	18	0.31	24	0.32
18.23	18	0.29	20	0.26

Fig. 2 Zero-shear rate viscosity and main relaxation time for 0.11 M CTAT solutions as a function of C_{SALT}/C_{CTAT} for: (□) KCl, (●) KBr, (△) K_2SO_4, (▼) (COONa)$_2$, (○) K_3PO_4. The dashed solid signals the end of each step.

CTAT concentration increases and so, the dynamical response moves to higher frequencies.

From Cole–Cole plots, deviations from the semicircle were observed at high frequencies, of the order of the inverse of the micellar breaking time, τ_{break}, indicating that these micellar solutions do not behave like a Maxwell fluid.[31] Similar results were observed with the other salts (as well as with 0.24 M CTAT solutions) at the temperatures examined (not shown). Values of viscoelastic data were fitted with the Granek–Cates model,[28] from which the ζ-values were determined. The ζ-values as a function of C_{SALT}/C_{CTAT} for the different systems examined fall in the range of 0.005 to 0.03, which indicates that these solutions are in the *fast-breaking* regime ($\zeta < 0.01$), regardless of the salt type and surfactant concentration (0.11 or 0.24 M).

Fig. 2 displays η_0 and τ_C as a function of C_{SALT}/C_{CTAT} at 30 °C for 0.11 M CTAT solutions containing the salts examined. For solutions with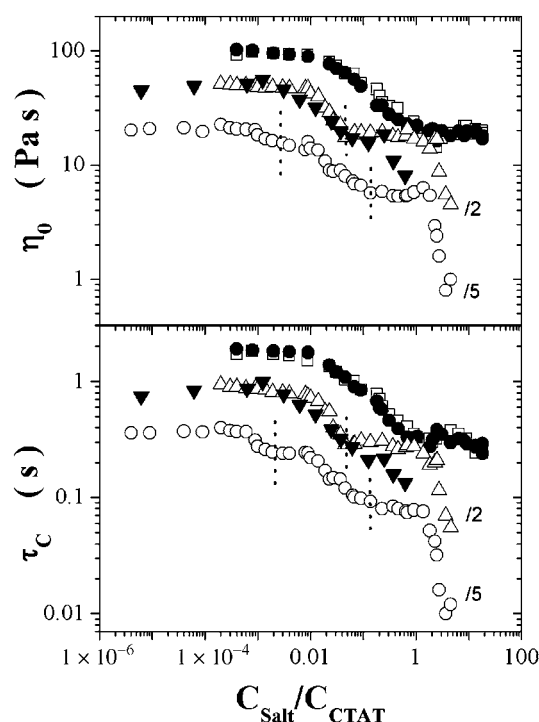 KBr and KCl, a plateau at low salt content (up to $C_{SALT}/C_{CTAT} \approx 0.009$ for the 0.11 M solutions) in both η_0 and τ_C, followed by a drop at intermediate salt concentrations ($0.0091 < C_{SALT}/C_{CTAT} < 0.7$ for the 0.11 M solutions), and another plateau at high salt concentrations ($C_{SALT}/C_{CTAT} > 0.7$ for the 0.11 M solutions) are observed. Notice that the micellar solutions with KCl and KBr follow the same patterns and have similar, but not equal, viscosity values for all C_{SALT}/C_{CTAT}. This is because both have mono-valent counterions (Cl$^-$ and Br$^-$), similar electronegativities (2.74 and 2.83) and sizes (1.95 and 1.81 Å).[33] However, it is noteworthy that the values of these viscoelastic parameters are consistently higher for solutions containing Cl$^-$ than those made with Br$^-$ ions in the whole range of salt/surfactant ratio (Table 1). With K_2SO_4 and (COONa)$_2$, four different regions (two *steps* and two *plateaus*) were observed. At low salt concentrations (up to $C_{SALT}/C_{CTAT} \approx 0.001$), a plateau is observed for both η_0 and τ_C. For moderate salt concentrations ($0.001 < C_{SALT}/C_{CTAT} < 0.1$), η_0 and τ_C decrease by about a third of the first-plateau value with increasing salt concentration. At salt contents higher than $C_{SALT}/C_{CTAT} = 0.1$, another plateau followed by a drastic fall in η_0 and τ_C is observed, *i.e.*, a second step comes up. Again and even though η_0 and τ_C are similar for both salts at identical concentrations, they are consistently larger for solutions containing SO$_4{}^{2-}$ than those containing C$_2$O$_4{}^{2-}$ (Table 1). For trivalent salts, three well-defined steps (three plateaus followed by three drops) in η_0 and τ_C are detected for a micellar solution containing 0.11 M of CTAT and K_3PO_4 as a function of the ratio C_{SALT}/C_{CTAT}. For the 0.11 M CTAT sample, the first plateau ends at a $C_{SALT}/C_{CTAT} \approx 6.8 \times 10^{-4}$ whereas the other two plateaus appear at $0.0036 < C_{SALT}/C_{CTAT}$

< 0.0091 and 0.14 < C_{SALT}/C_{CTAT} < 0.91, respectively. It is important to notice that these three steps correspond to the changes of the ionisation of the phosphate present (as depicted in Fig. 6).

Close examination of Table 1 reveals that both η_0 and τ_C depend on the anionic species (counterions) at the interface; in fact, the influence of the anions increases in the order: PO_4^{3-} < SO_4^{2-} < $C_2O_4^{2-}$ < HPO_4^{2-} < HSO_4^- < $C_2O_4H^-$ < $H_2PO_4^-$ < Cl^- < Br^-, which follows the Hofmeister series of salting-in.[27,34,35] Scheme 1 shows the Hofmeister series followed by anionic counterions with respect to their affinity to the trimethylammonium headgroup (CTA^+). For anions, the Hofmeister series follows the order $citrate^{3-}$ > SO_4^{2-} = $tartrate^{2-}$ > HPO_4^{2-} > CrO_4^{2-} > $acetate^-$ > HCO_3^- > Cl^- > NO_3^- > ClO_3^-, the most salting-out agents lie on the left while the most salting-in lie on the right.[27] This classification turned out to be valid for most salting-out agents lying on the left, while it holds for the most salting-in ones lying on the right. This classification turned out to be valid for a great number of processes in biology[36] as well as surface chemistry.[37,38] However, and in spite of the huge amount of experimental data, it is still difficult to clearly explain the ion-specific effects, mainly because they simultaneously result from several interactions such as dielectric, steric, and dispersion forces, and also from specific hydration of ions at interfaces.[39] It is noteworthy that recently, Shrestha et al.[40] reported that the linear viscoelastic properties of wormlike micelles composed of mixed amino acid surfactant/nonionic surfactant follow the Hofmeister series.

Fig. 3 shows Arrhenius plots of η_0 and τ_C for 0.11 M CTAT solutions containing different C_{SALT}/C_{CTAT} with K_2SO_4 as the salt, which demonstrate that these solutions exhibit the typical viscosity drop with increasing temperature and follow the Arrhenius dependence. The activation energy estimated from the slope of these plots increases for low ratios of C_{SALT}/C_{CTAT} up to a maximum around 0.5, and then it decreases at higher C_{SALT}/C_{CTAT} ratios. Calculated activation energies for various C_{SALT}/C_{CTAT} ratios (0, 0.1, 0.5, 1 and 5) are 19.2, 22.12, 25.03, 19.80 and 9.33 kcal mol^{-1} K^{-1}, respectively. The data confirm that the C_{SALT}/C_{CTAT} ratio indeed affects the hydrophobe dissociation kinetics. A higher activation energy indicates stronger association junctions. The maximum activation energy obtained at C_{SALT}/C_{CTAT} = 0.5 indicates that at this salt content, the solution forms the strongest hydrophobic junctions, possibly arising from the optimal aggregation number in each junction. It is interesting that the solution with C_{SALT}/C_{CTAT} = 0.5 generates the highest activation energy but has lower solution viscosity
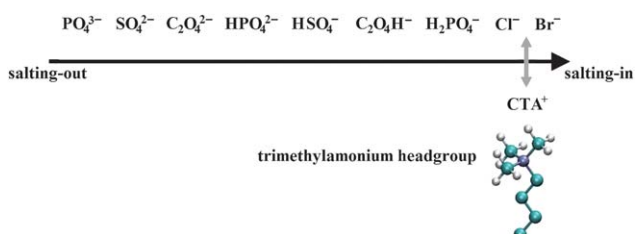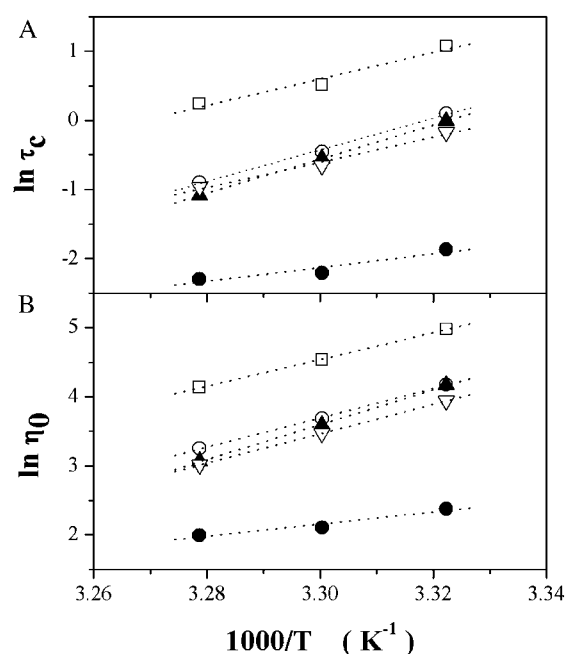
Fig. 3 Arrhenius plots for (A) zero-shear rate complex viscosity and (B) main relaxation time of 0.11 M solutions containing K_2SO_4 as a function of C_{SALT}/C_{CTAT}: (□) 0; (○) 0.1; (▲) 0.5; (▽) 1 and (●) 5.

than the C_{SALT}/C_{CTAT} = 5. Thus, the decrease in the activation energy as the ratio C_{SALT}/C_{CTAT} increases from 0.5 to 5 suggests that the chain conformation is influenced by the hydrophobic association and that the activation energy is not totally independent of chain conformation, as assumed by the transient network theory.[41] The dependences of η_0 and τ_C with temperature were not investigated with the other salts. Brown has proposed that the magnitude of the viscosity is a function of chain conformation and the hydrophobe size.[42]

Fig. 4 depicts the reduced shear flow curves for 0.11 M CTAT solutions containing increasing concentrations of K_3PO_4. Newtonian behavior is detected at low reduced shear rates ($\dot{\gamma}\tau_C \leq 1$), where all data collapse in a single line. For $\dot{\gamma}\tau_C > 1$, a stress plateau develops. The plateau region is wider for low C_{SALT}/C_{CTAT}, and the span of the plateau region becomes increasingly narrower as C_{SALT}/C_{CTAT} is increased. In all cases, a second Newtonian region is detected at reduced shear-rates higher than $\dot{\gamma}_{c2}\tau_C$. Notice that the transition into the stress plateau is sharper for solutions with low C_{SALT}/C_{CTAT}, but it becomes smoother as the C_{SALT}/C_{CTAT} augments. The stress plateau occurs at $0.4 \leq \sigma/G_0 \leq 1$ as C_{SALT}/C_{CTAT} is increased, which differs from the value of 0.67 predicted by the Cates model.[8,31,43] In the inset, the variation of the stress plateau with C_{SALT}/C_{CTAT} depicts three steps. The pattern followed by the stress plateau with C_{SALT}/C_{CTAT} is the inverse of the mirror image of the pattern observed for η_0 (Fig. 2). For salts with different valence, we observed a similar behavior (Fig. S1 and S2†). The predictions of the BMP-model (solid lines) with the parameter obtained experimentally reported in Table 2 reproduce well the experimental data.

Fig. 5 displays the shear stress growth upon inception of flow as a function of the applied shear rate for a 0.11 M CTAT

Scheme 1 Hofmeister series that shows the ordering of anionic counterions with respect to their affinity for the trimethylammonium headgroup (CTA^+). The arrow means strong interactions.
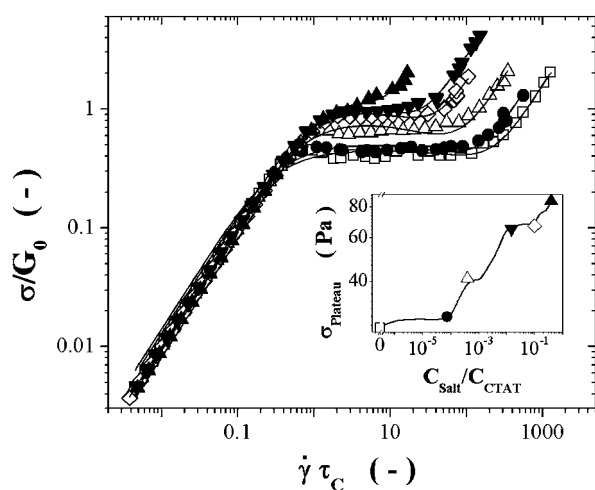
Fig. 4 Reduced shear stress *versus* reduced shear rate for 0.11 M solutions containing K_3PO_4 as function of C_{SALT}/C_{CTAT}: (□) 0, (●) 0.0001, (△) 0.001, (▼) 0.01, (◇) 0.1 and (▲) 1. Inset: shear stress plateau as a function of C_{SALT}/C_{CTAT}. Solid lines represent the best fit of the BMP Model.[37]

solution with K_2SO_4 ($C_{SALT}/C_{CTAT} = 0.1$). At low shear rates, *i.e.*, within the Newtonian region (see inset), the stress growth can be reproduced with the Maxwell model and the value of τ_C obtained from oscillatory experiments (Table 1). As the applied shear rate approaches the multi-valued region, *i.e.*, $\dot{\gamma}\tau_C \rightarrow 1$, stress overshoots and oscillations are detected and many relaxation times are required to achieve steady state. Notice that the overshoots appear at *ca.* $\dot{\gamma}\tau_C \approx 0.5$ (this is observed with all the samples examined). Also, as the shear rate is increased, the period of the oscillations becomes longer until they disappear completely as the shear rate approaches the second critical shear rate ($\dot{\gamma}_{c2}$), where the high-shear rate Newtonian branch appears. Similar results were detected at other C_{SALT}/C_{CTAT} with the five salts used. The inset depicts the stress relaxation after cessation of steady shear flow for a 0.11 M CTAT solution with K_2SO_4 ($C_{SALT}/C_{CTAT} = 0.1$). For applied shear rates smaller than the onset of the plateau stress region (*i.e.*, $\dot{\gamma}\tau_C < 1$), the stress is single exponential and it can be reproduced with the Maxwell model and the experimental values of τ_C. For $\dot{\gamma} \geq \dot{\gamma}_{c1}$, the relaxation curves are no longer single exponential but exhibit fast and slow decays with a transition region between them. The fast relaxation time is sensitive to the applied shear rate, *i.e.*, it depends on the steady viscosity prior to relaxation, whereas the slow mode is mono-exponential with a decay constant equal to the Maxwell relaxation time (τ_C). Therefore, at long times, relaxation decays follow straight lines with identical slopes, the ordinates of which depend on the magnitude of the steady state viscosity, as expected.[44] Similar results were attained at other C_{SALT}/C_{CTAT} and with the five salts used.

Discussion and conclusions

In water, CTAT forms micelles that have a small surface charge but large Debye screening length due to the strong binding and weak dissociation of the counterions. As a result, CTAT micelles grow slowly in the concentration range of 1.32–15.4 mM and get

Table 2 Parameters obtained from the best fit to the BMP-model[a] ($k_0\lambda$ and μ_1) for a micellar solution containing 5 wt% CTAT as a function of the ratio C_{SALT}/C_{CTAT}, here φ_0 and φ_∞ were obtained from independent rheological measurements

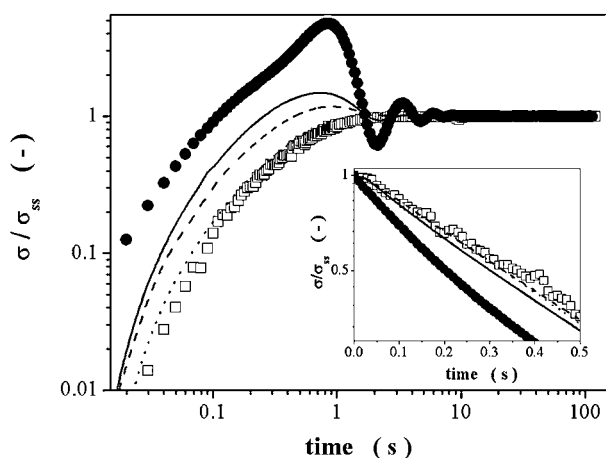| C_{SALT}/C_{CTAT}	K$_3$PO$_4$				K$_2$SO$_4$				KBr			
	φ_0/Pa^{-1} s^{-1}	φ_∞/Pa^{-1} s^{-1}	$k_0\lambda$/s Pa^{-1}	μ_1/s	φ_0/Pa^{-1} s^{-1}	φ_∞/Pa^{-1} s^{-1}	$k_0\lambda$/s Pa^{-1}	μ_1/s	φ_0/Pa^{-1} s^{-1}	φ_∞/Pa^{-1} s^{-1}	$k_0\lambda$/s Pa^{-1}	μ_1/s
0	0.007	0.01	0.710	639.1	0.007	0.01	0.756	601.3	0.007	0.01	0.745	640.5
0.0001	0.008	0.02	0.771	410.8	—	—	—	—	—	—	—	—
0.001	0.008	0.05	0.927	169.5	0.015	0.03	0.890	282.7	0.008	0.02	0.811	446.5
0.01	0.012	0.10	1.009	60.75	0.028	0.05	0.782	87.62	—	—	—	—
0.05	—	—	—	—	0.041	0.07	0.754	41.21	0.019	0.10	0.825	44.11
0.1	0.009	0.30	1.075	36.34	0.025	0.10	1.067	42.27	0.010	0.10	0.776	28.66
1	0.019	1.00	1.234	9.399	0.027	0.12	0.956	36.29	0.008	0.10	0.860	38.17
5	—	—	—	—	0.014	0.50	0.952	25.08				

[a] See ref. 37 for more details.

Fig. 5 Stress growth upon inception of flow as a function of the applied shear rate for a 0.11 M CTAT solution with K_2SO_4 ($C_{SALT}/C_{CTAT} = 0.1$): ($\square$) 0.04 s^{-1}, (dotted line) 0.1 s^{-1}, (dashed line) 0.5 s^{-1}, (solid line) 3 s^{-1}, and ($\bullet$) 10 s^{-1}. Inset: stress relaxation after cessation of steady shear flow.

entangled beyond an overlap concentration of 15.4 mM.[12] Above this concentration and up to *ca.* 0.55 M, CTAT micellar solutions are strongly viscoelastic.[11] Moreover, it was shown elsewhere that the relaxation of salt-free CTAT polymer-like micellar solutions is kinetic-controlled (*fast breaking* regime), *i.e.*, the linear viscoelastic properties follow Maxwell behavior up to moderate frequencies ($\omega\tau_C \approx 1$), and that they exhibit shear-banding flow in the concentration range of 0.044 to 0.55 M.[11]

Evidence reported in the literature indicates that fast breaking ($\tau_{Break}/\tau_{Rep} \ll 1$) is a necessary condition for shear banding flow.[8,13,43–45] Also, $\dot{\gamma}_{c1}$ and $\dot{\gamma}_{c2}$ appear to be related to the cross-over frequencies of G' and G'' in the low and high frequency regions, *i.e.*, to the inverses of the reptation (long relaxation) and Rouse times. Mcleish and Ball,[45] based on the Doi–Edwards reptation theory for polymer solutions, proposed that these characteristic times provide two conditions in the σ–$\dot{\gamma}$ relationship that give rise to shear banding flow. However, for flexible polymers, these characteristic times depend strongly on molar mass ($\tau_{Rep} \propto M^3$ and $\tau_{Rouse} \propto M^2$), and hence, molar mass (size) polydispersity masks the discontinuity in σ *versus* $\dot{\gamma}$. Wormlike micellar solutions have a broad size distribution but because of the chain breaking and recombination processes that average the chain length distribution, they behave as highly monodisperse systems in the fast breaking regime.[31] As a result, fast-breaking wormlike micellar solutions follow Maxwell behavior with a single relaxation time in the linear viscoelastic regime and shear banding in steady shear flow.

Addition of salt does not shift the CTAT micellar solutions to the slow breaking regime. Moreover, these micellar solutions follow the Maxwell model up to moderate reduced frequencies ($\omega\tau_C \approx 1$) and a superposition of temperature–time–surfactant concentration and salt concentration is possible with the five salts examined (Fig. 1). In fact, the values of ζ (<0.03) indicate that relaxation occurs mostly by micellar *breaking* and *recombination* and that τ_{Break} steadily decreases as C_{SALT}/C_{CTAT} increases. Hence, as expected, shear-banding flow is observed in all the micellar solutions examined here, regardless of the type and

concentration of salt used (Fig. 4). The value of the stress plateau, however, depends on salt type and concentration (inset in Fig. 4). In fact, the plateau stress evolves continuously with increasing salt concentration until it vanishes. Notice that $\sigma_{Plateau}/G_0$ increases with increasing C_{SALT}/C_{CTAT} from values lower than the theoretical one (0.67) to larger ones (Fig. 4). Elsewhere it was reported that in salt-free micellar solutions of surfactants with bromide counterions, the electrostatic interactions lower considerably the value of $\sigma_{Plateau}/G_0$, and that in screened systems upon addition of salt, this value increases above 0.67.[44] Hence, our results suggest that the main effect of adding salts to the CTAT micellar solutions is to screen of electrostatic interactions but other factors, such as ion-specific interactions, may play a role.

The long transients and oscillations that typically accompany shear-banding flow were also detected in all the systems examined here (Fig. 5). The overshoots, undershoots and oscillations appear at the onset of the stress plateau and become more pronounced as the shear rate is increased above $\dot{\gamma}_{c1}$. As the shear rate approaches $\dot{\gamma}_{c2}$, the period of the oscillations becomes longer until the oscillations disappear at $\dot{\gamma} > \dot{\gamma}_{c2}$. Berret and Porte[46] have concluded that the oscillations and long transients around shear banding resemble the kinetics of nucleation and growth of a second phase, similar to phenomena occurring in equilibrium first-order phase transitions. Notice that the stress growth is nearly Maxwellian when the shear rate is within the Newtonian regions (Fig. 5). Recent results reported by our group[47] indicate that indeed shear banding flow is due to a non-equilibrium first-order phase transition, in which a critical point develops as the shear-banding region vanishes.

Another feature that has been observed when shear banding occurs is the presence of more than one relaxation mechanism upon cessation of steady shear flow. A slow, a transition and a fast relaxation mechanisms have been distinguished when the flow is suddenly stopped after the sample is subjected to a shear rate equal to or larger than $\dot{\gamma}_{c1}$.[44] Fig. 5 demonstrates that this is the case in all the samples examined here. When the applied shear rate is smaller than $\dot{\gamma}_{c1}$, the relaxation is single-exponential and it can be reproduced with the Maxwell model and the experimental value of τ_C. However, as the shear rate approaches $\dot{\gamma}_{c1}$, an incipient fast relaxation mode appears, which becomes more pronounced as the shear rate surpasses $\dot{\gamma}_{c1}$. Unfortunately, relaxation experiments could not been performed at shear rates within the high-shear rate Newtonian branch. Yet, results reported for DTAB/Na salicylate wormlike micellar solutions indicate that the relaxation becomes single-exponential again for $\dot{\gamma} > \dot{\gamma}_{c2}$ with a slope similar to the fast relaxation mode.[43] The similarities of the relaxation modes in the low- and high-shear rate bands with the slow and fast relaxation mechanisms in the shear-banding region suggest the presence of two bands: one made with the original micellar solutions and other with a shear-induced oriented fluid phase. As a matter of fact, two bands have clearly identified in several wormlike micellar solutions by rheo-optics and other techniques.[20,48–50]

In contrast to many surfactant systems that first exhibit a rise up to a maximum in viscosity with increasing salt content due to micellar growth, the CTAT system depicts a step-like decrease with increasing salt content (Fig. 2). Also, the main relaxation time (Fig. 2) decreases steadily with increasing C_{SALT}/C_{CTAT}

with the five salts studied. These results suggest a continuous decrease in micellar length with increasing salt content causing a fast relaxation (the decrease in τ_{Break}) and a drop in viscosity. However, the behavior of the plateau modulus (Table 1) indicates that the structure of entangled micelles is maintained. A most likely explanation is an increasingly branching occurring in the presence of salt due to the screening of electrostatic interactions. In this situation, the relaxation process is speeded up by the formation of crosslinks that yield a modification of the terminal relaxation time.

Narayanan and collaborators[14] reported similar results in wormlike micellar solutions of CTAHCN upon addition of NaBr and sodium acetate, that is, η_0 and τ_C decreased several-fold upon increasing the salt content, whereas G_0 was only slightly affected. HCN⁻ is a counterion that binds strongly to the micelle surface, and so, Br⁻ and CH_3COO^- ions cannot exchange with HCN ions from the micelles. Hence, these authors concluded that the effect of adding this salt is purely electrostatic screening and explained their results in terms of increasing branching upon addition of salt.[14] It is noteworthy that these authors did not observe the second viscosity and terminal time plateaus reported here with KCl or KBr (Fig. 2), probably because they did not examine very high salt contents. In fact, the patterns that η_0 and τ_C follow with increasing $(COONa)_2$, K_2SO_4 and K_3PO_4 have not been reported in the literature as far as we know.

It is well known that salts from strong (sulfuric) or weak (oxalic and phosphoric) acids can dissociate into several species with increasing salt content in water. Here we propose that the appearance of the η_0 and τ_C plateaus (Fig. 2) is related to the presence of the different counterions from the equilibrium dissociation of the salts, which produce different anionic species that modify the interface. K_3PO_4 produces $H_2PO_4^-$, HPO_4^{2-} and PO_4^{3-} upon increasing concentration; the pK_a's of H_3PO_4 are 2.13, 7.21 and 12.32, respectively.[51] To demonstrate that the different ions are present here, the pH of K_3PO_4 was measured in water and in 0.11 M CTAT aqueous solutions as a function of salt concentration (Fig. 6). The pH's of the aqueous and of the micellar solutions increase with increasing salt content but the later is consistently higher than that in water. This interference may be due to the presence of CTAT, which is a salt of a weak base and strong acid (p-toluene sulfonic acid). Hence, we are in the situation of a weak base group (CTA⁺) and a weak acid group ($H_2PO_4^-$ or HPO_4^{2-}) that, even though they are not in the same molecule, are similar to that situation in which an amphoteric molecule is present.[52] In this case, the isoelectric point is the average pH of the pK_a's of the acid and the basic groups. Elsewhere we measured the pK_b of DTAOH (= 2.89), which gives a pK_a of 11.1.[53] Assuming that the pK_a of CTAOH is similar, we have that the isoelectric point with $H_2PO_4^-$ is (2.13 + 11.1)/2 = 6.65 and that with HPO_4^{2-} is 9.15.

Clearly, the salt concentration ranges at which η_0 and τ_C (Fig. 2) plateaus appear are within the salt concentrations at which these isoelectric points occur (shown by the dotted lines in Fig. 6), and they indicate the pH's at which the different ions dominate (cf. Fig. S1) (ESI †). It is interesting that Mukerjee and Banerjee[54] reported a modification of the surface pH in surfactant aggregates with respect to the bulk of the intermicellar solution and interpreted these changes in terms of the electrical surface potential and the corresponding changes of the intrinsic
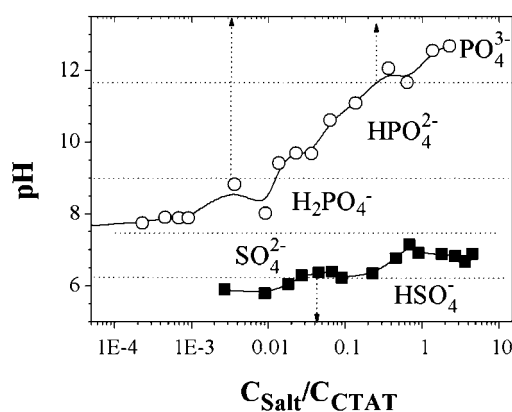

Fig. 6 pH of 0.11 M CTAT aqueous solutions as a function of C_{CSALT}/C_{CTAT} containing K_3PO_4 (○) or K_2SO_4 (■).

value of the pK_a of the probe used. Also, there is a tendency for the accumulation of OH⁻ ions at the cationic micellar surface, in competence with other counterions—this fact is used in micellar catalysis.[53] Hence, the counterions, which are weak acid groups and are in the Stern layer, encounter a more basic environment than that of the intermicellar solution and, as a result, the pH of the micellar solution shifts to higher values compared to that in the surfactant-free salt solution. Hence, we propose that the step behavior observed in the viscosity and relaxation time (Fig. 2) is related to the different electrostatic screening of the salt valence.

A similar situation takes place with K_2SO_4 and $Na_2C_2O_4$. The second η_0 plateau appears at C_{SALT} between 5 and 6 mM and disappears at around 10 mM (Fig. 2). The pH of micellar solutions with this salt increases slightly (pH > 6.5) at C_{SALT} around 8 mM (see Fig. 6). This suggests that for pH below ca. 8 mM, HSO_4^- ions dominate and that SO_4^{2-} ions are the dominant species for larger salt concentrations. For this salt, the pK_a of HSO_4^- is 1.92.[51] Again, assuming that the pK_a of CTAOH is 11.1, the pH of the isoelectric point for this system is (1.92 + 11.1)/2 = 6.5, which coincides remarkably well with the pH at which SO_4^{2-} begin to dominate. Notice that $(COONa)_2$ is dissociated completely in water in order to generate $C_2O_4^{2-}$ ions, which hydrolyse in water to generate $C_2O_4H^-$. However it is important to notice that $H_2C_2O_4$ is very difficult to obtain.

It is also significant that η_0 (and τ_C) begins to drop at a KCl (or KBr) concentration of 0.001 M. According to the Debye–Hückel approximation, the extent of the double layer at 30 °C and in a 0.001 M mono-valence salt solution is ca. 1 nm.[55] Assuming that this extent of the double layer is the minimum required for micelles to approach each other and to start forming interconnections, then one expects that lower salt concentrations are required with a di- or tri-valence salt. Again, with the same approximation, the same thickness of the double layer is achieved at 0.00023 M and at 0.00008 M with the di- and tri-valence salts, respectively. Examination of Fig. 2 reveals that indeed the concentration at which the first drop in viscosity is noticed shifts to lower values with K_2SO_4 and $(COONa)_2$ (0.00015 M), and also with K_3PO_4 (0.000077 M), which are very similar to the predicted ones, i.e., they follow the screening length of the system. Finally, it is striking that the plateau in viscosity and main relaxation time form at same salt concentrations independently of the surfactant concentration.

Moreover, the unusual behavior observed on the shear flow curves (particularly in the zero-shear viscosity) was determined by the anionic (counterion) species at the interface. But in spite of the large amount of experimental data, it is still very difficult to explain clearly these specific ion effects, mainly because they result not only from several interactions such as dielectric, steric, and dispersion forces, but also from a specific hydration of ions at interfaces.[56] Commonly one considers the ions as isolated species in water, but they interact with one another (except in very dilute solutions, where Debye–Hückel expressions are strictly valid) and with their neighboring surfaces. Consequently, the specificity not only depends on the type of ion considered, but also on the counterion or on the chemical composition of the surface involved. Hence, it is important to define a better classification or Hofmeister series of headgroups together with a predictive theory of interactions between different types of ions and headgroups.

Experimental section

CTAT (98%+ pure from SIGMA) was re-crystallized from chloroform (Fermont) and ether (Fermont). The salts were 99% pure from Fluka. Water was bi-distilled and de-ionized. Samples with surfactant concentrations of 0.11 and 0.24 M were made by dissolving the CTAT in the salt solution of the appropriate concentration to give constant values of C_{SALT}/C_{CTAT} (0.009 < C_{SALT}/C_{CTAT} < 18.14) and heating to about 50 °C for one to 24 hours; then they were left standing at the temperature of measurement for one week.

Steady and unsteady simple shear as well as small-amplitude oscillatory shear measurements were performed at 30 °C in a Rheometrics Dynamic Stress rheometer RS-5 with a cone-and-plate geometry with a diameter of 40 mm and an angle of 0.0384 radian (2.2°) and in a TA ARES rheometer with a cone-and-plate geometry of 0.0399 radian and 50 mm in diameter. An environmental control unit was used during the measurements to prevent the evaporation of the solvent.

The pH of the CTAT/salt solutions was measured in an Oakton pH/conductivity bench meter 510. The pH meter was calibrated with buffer solutions of pH = 4, 7 and 10 from J.T. Baker.

Acknowledgements

References

1 J. N. Israelachvilli, *Intermolecular and Surface Forces*, Academic Press, Inc., San Diego, 2nd edn, 1992.
2 M. E. Cates, *Macromolecules*, 1987, **20**, 2289.
3 H. Rehage and H. Hoffmann, *J. Phys. Chem.*, 1988, **92**, 4712.
4 T. Shikata and H. Hirata, *Langmuir*, 1989, **5**, 398.
5 B. K. Mishra, S. D. Samant, P. Pradhan, S. B. Mishra and C. Manohar, *Langmuir*, 1993, **9**, 894.
6 H. Hoffmann, C. Thunig, P. Schmiedel, U. Munkert and W. Ulbricht, *Tenside, Surfactants, Deterg.*, 1994, **31**, 389; H. Hoffmann, in *Structure and Flow in Surfactant Solutions*, ed. C. A. Herb, R. K. Prud'home, ACS Symposium Series, 1994, vol. 578, p. 2.
7 A. Khatory, F. Kern, F. Lequeux, J. Appell, G. Porte, N. Morie, A. Ott and W. Urbach, *Langmuir*, 1993, **9**, 933.
8 A. Ait Ali and R. Makhloufi, *Phys. Rev. E: Stat. Phys., Plasmas, Fluids, Relat. Interdiscip. Top.*, 1997, **56**, 4474; A. Ait Ali and R. Makhloufi, *J. Rheol. (Melville, NY, U. S.)*, 1997, **41**, 307; A. Ait Ali and R. Makhloufi, *Colloid Polym. Sci.*, 1999, **277**, 270.
9 S. E. Imai, E. Kunimoto and T. Shikata, *J. Soc. Rheol. Jpn.*, 2000, **28**, 61; S. E. Imai, E. Kunimoto and T. Shikata, *J. Soc. Rheol. Jpn.*, 2000, **28**, 67; S. E. Imai and T. Shikata, *J. Colloid Interface Sci.*, 2001, **244**, 399.
10 T. Shikata, H. Hirata and T. Kotaka, *Langmuir*, 1987, **3**, 1081; T. Shikata, H. Hirata and T. Kotaka, *Langmuir*, 1988, **4**, 354.
11 J. F. A. Soltero, J. E. Puig, O. Manero and P. Schulz, *Langmuir*, 1995, **11**, 3337; J. F. A. Soltero and J. E. Puig, *Langmuir*, 1996, **12**, 2654; J. F. A. Soltero, F. Bautista, J. E. Puig and O. Manero, *Langmuir*, 1999, **15**, 1604.
12 M. Carver, T. L. Smith, J. C. Gee, A. Delichere, E. Caponnetti and L. J. Magid, *Langmuir*, 1996, **12**, 691.
13 P. A. Hassan, S. J. Candau, F. Kern and C. Manohar, *Langmuir*, 1998, **14**, 6025; P. A. Hassan, B. S. Valaulikar, C. Manohar, F. Kern, L. Bourdieu and S. J. Candau, *Langmuir*, 1996, **12**, 4350.
14 R. Oda, J. Narayanan, P. A. Hassan, C. Manohar, R. A. Salkar, F. Kern and S. J. Candau, *Langmuir*, 1998, **14**, 4364; J. Nayaranan, C. Manohar, F. Kern, F. Lequeux and S. J. Candau, *Langmuir*, 1997, **13**, 398; J. Nayaranan, C. Manohar, F. Kern, F. Lequeux and S. J. Candau, *Langmuir*, 1997, **13**, 5235.
15 N. A. Mazer, G. B. Benedeck and M. C. Carey, *J. Phys. Chem.*, 1976, **80**, 1075.
16 H. Hoffmann, H. Rehage, G. Platz, W. Schorr, H. Thurn and W. Ulbricht, *Colloid Polym. Sci.*, 1982, **260**, 1042; H. Rehage and H. Hoffmann, *Mol. Phys.*, 1991, **74**, 933.
17 G. Porte and J. Appell, *J. Phys. Chem.*, 1981, **85**, 2511.
18 F. Kern, P. Lemarechal, S. J. Candau and M. E. Cates, *Langmuir*, 1992, **8**, 437; A. Khatory, F. Lequeux, F. Kern and S. J. Candau, *Langmuir*, 1993, **9**, 1456.
19 R. T. Buwalda, M. C. A. Stuart and J. B. F. N. Engberts, *Langmuir*, 2000, **16**, 6780.
20 J. F. Berret, D. C. Roux and G. Porte, *J. Phys. II*, 1994, **4**, 1261; J. F. Berret, G. Porte and J. P. Decruppe, *Phys. Rev. E: Stat. Phys., Plasmas, Fluids, Relat. Interdiscip. Top.*, 1997, **55**, 1668.
21 S. Lerouge, J. P. Decruppe and C. Humbert, *Phys. Rev. Lett.*, 1998, **81**, 5457.
22 F. Kern, R. Zana and S. J. Candau, *Langmuir*, 1991, **7**, 1344; F. Kern, F. Lequeux, R. Zana and S. J. Candau, *Langmuir*, 1994, **14**, 1710.
23 I. A. Kadoma and J. W. van Egmond, *Langmuir*, 1997, **13**, 4551; I. A. Kadoma and J. W. van Egmond, *Phys. Rev. Lett.*, 1996, **76**(23), 4432.
24 G. Porte, R. Gomati, O. El Haitami, J. Appell and J. Marignan, *J. Phys. Chem.*, 1986, **90**, 746; A. Khatory, F. Kern, F. Lequeux, J. Appell, G. Porte, N. Morie, A. Ott and W. Urbach, *Langmuir*, 1993, **9**, 933.
25 M. S. Turner and M. E. Cates, *J. Phys.: Condens. Matter*, 1992, **4**, 3719.
26 T. Shikata, M. Shiokawa and S. J. Imai, *J. Colloid Interface Sci.*, 2003, **259**, 367.
27 Y. Zhang and P. S. Cremer, *Curr. Opin. Colloid Interface Sci.*, 2006, **10**, 658.
28 R. Granek and M. E. Cates, *J. Chem. Phys.*, 1992, **96**, 4758.
29 F. Bautista, J. M. de Santos, J. E. Puig and O. Manero, *J. Non-Newtonian Fluid Mech.*, 1999, **80**, 93; F. Bautista, J. F. A. Soltero, O. Manero and J. E. Puig, *J. Phys. Chem. B*, 2002, **106**, 13018.
30 M. Doi and S. F. Edwards, *The Theory of Polymer Dynamics*, Clarendon Press, Oxford, U.K. 1986.
31 M. E. Cates and S. J. Candau, *J. Phys.: Condens. Matter*, 1990, **2**, 6869; M. E. Cates, *J. Phys.: Condens. Matter*, 1996, **8**, 9167.
32 V. Schmitt and F. Lequeux, *J. Phys. II*, 1995, **5**, 193.
33 R. B. Heslop and P. L. Robinson, *Inorganic Chemistry*, Elsevier, Amsterdam, 3rd ed, 1967; *Valencia y Estructura Molecular*, ed. E. Cartmell and G. W. A. Fowles, Reverté, Barcelona, 1967.
34 L. Gaillon, J. Lelievere and R. Gaboriaud, *J. Colloid Interface Sci.*, 1999, **213**, 287.
35 F. Hofmeister, *Arch. Exp. Pathol. Pharmakol.*, 1888, **24**, 247.
36 W. Kunz, P. Lo Nostro and B. W. Ninham, *Curr. Opin. Colloid Interface Sci.*, 2004, **9**, 1.
37 H. Schott and A. E. Royce, *J. Pharm. Sci.*, 1983, **72**(12), 1427.
38 C. Holtzscherer and F. Candau, *J. Colloid Interface Sci.*, 1988, **125**(1), 97.
39 P. Jungwirth and D. J. Tobias, *Chem. Rev.*, 2006, **106**, 83.
40 R. G. Shrestha, C. Rodriguez-Abreu and K. Aramaki, *J. Oleo Sci.*, 2009, **58**, 243.

41 F. Tanaka, *Langmuir*, 2010, **26**, 5374.
42 G. Brown and A. Chakrabarti, *J. Chem. Phys.*, 1992, **96**, 3251.
43 N. A. Spenley, M. E. Cates and T. C. B. McLeish, *Phys. Rev. Lett.*, 1993, **71**, 939; M. E. Cates, T. C. B. McLeish and G. Marrucci, *Europhys. Lett.*, 1993, **21**, 451.
44 J. I. Escalante, E. R. Macías, F. Bautista, J. H. Pérez-López, J. F. A. Soltero, J. E. Puig and O. Manero, *Langmuir*, 2003, **19**, 6663; J. E. Puig, J. I. Escalante, E. R. Macías, J. F. A. Soltero, F. Bautista and O. Manero, *Recent Res. Dev. Surf. Colloids*, 2004, **1**, 145–167.
45 T. C. B. McLeish and R. C. Ball, *J. Polym. Sci., Polym. Phys. Ed.*, 1986, **24**, 1735.
46 J. F. Berret and G. Porte, *Phys. Rev. E: Stat. Phys., Plasmas, Fluids, Relat. Interdiscip. Top.*, 1999, **60**, 4268.
47 F. Bautista, M. Muñoz, J. Castillo-Tejas, J. H. Pérez-López, J. E. Puig and O. Manero, *J. Phys. Chem. B*, 2009, **113**(50), 16101–16109.
48 V. Schmitt, F. Lequeux, A. Pousse and D. Roux, *Langmuir*, 1994, **10**, 955; V. Schmitt, F. Shosseler and F. Lequeux, *Europhys. Lett.*, 1995, **30**, 31.
49 E. Cappelaere, R. Cressely, R. Makhloufi and F. Kern, *Rheol. Acta*, 1994, **33**, 431; E. Cappelaere, R. Cressely and J.-P. Decruppe, *Colloids Surf.*, 1995, **104**, 353–374; J. P. Decruppe, R. Cressely, R. Makhloufi and E. Cappelaere, *Colloid Polym. Sci.*, 1995, **273**, 346.
50 E. Fisher and P. T. Callaghan, *Europhys. Lett.*, 2000, **50**, 803; E. Fisher and P. T. Callaghan, *Phys. Rev. E: Stat., Nonlinear, Soft Matter Phys.*, 2001, **64**, 11501.
51 *Handbook of Chemistry and Physics*, ed. D. R. Lide, CRC Pub. Co., Boca Raton, FL, 76th edn, 1995.
52 S. Glasstone, *Introduction to Electrochemistry*, Van Nostrand, Princeton, 1960, p. 628.
53 M. A. Morini, R. M. Minardi, P. C. Schulz, J. E. Puig and M. E. Hernández-Vargas, *Colloids Surf., A*, 1995, **109**, 37; M. A. Morini, P. C. Schulz and J. E. Puig, *Colloid Polym. Sci.*, 1996, **274**, 662.
54 P. Mukerjee and K. Banerjee, *J. Phys. Chem.*, 1964, **68**, 3567.
55 R. J. Hunter, *Foundations of Colloid Science*, Oxford Univ. Press., New York, 1989, vol. 1, p. 332.
56 P. Jungwirth and D. J. Tobias, *Chem. Rev.*, 2006, **106**, 83.